Analysis of charge-injection characteristics at electrode-organic interfaces: Case study of transition-metal oxides

Z. B. Wang,* M. G. Helander, M. T. Greiner, J. Qiu, and Z. H. Lu†
Department of Materials Science and Engineering, University of Toronto, 184 College Street, Toronto, Ontario, Canada M5S 3E4
(Received 16 August 2009; revised manuscript received 19 October 2009; published 18 December 2009)

The formation of resistance-free or Ohmic contacts at metal/organic interfaces remains a significant challenge for achieving high-performance organic electronic devices such as organic light-emitting diodes. Several oxides have recently been reported to yield extremely low-voltage devices and thus have excited a renewed interest in developing the next generation of contacting electrodes. In this paper, major metal oxides, CuO, Cu_2O, Ni_2O_3, Co_3O_4, WO_3, MoO_3, V_2O_5, and indium tin oxide, have been systematically studied to compare their relative performance as hole injection anodes, as well as to provide an experimental database for theoretical analysis of current-voltage (*IV*) characteristics with a diverse range of injection barrier heights. Contrary to previous reports in the literature, none of the oxides studied in this work were found to form a true Ohmic contact with commonly used hole transport layers, such as N,N-diphenyl-N, N-bis-1-naphthyl-1–1-biphenyl-4,4-diamine (α-NPD). This discrepancy is attributed to incorrect *IV* data analysis of the quasi-Ohmic injection regime—the region in between space-charge limited current (SCLC) and injection limited current (ILC)—in previous studies. It is found that the quasi-Ohmic regime is much larger (i.e., covers a greater range of injection barrier height) than has previously been expected. A criterion that defines Ohmic, quasi-Ohmic, and injection limited contacts has been quantified based on a time-domain simulation of charge transport across α-NPD single-carrier devices. This criterion includes the effects of the electric field dependent mobility, organic layer thickness, and charge-injection barrier height. The effects of the built-in potential on the *IV* characteristics are also evaluated. A barrier-thickness-voltage "phase" diagram that defines the regions of SCLC, quasi-Ohmic, and ILC for α-NPD is presented.

DOI: 10.1103/PhysRevB.80.235325 PACS number(s): 73.40.Sx, 72.80.Le

I. INTRODUCTION

Organic semiconductors contain almost no *intrinsic* charge carriers due to their weak intermolecular coupling. In order to enhance the performance of organic electronic devices such as organic light-emitting diodes (OLEDs), one has to increase the *extrinsic* carrier concentration. Therefore, improving the injection of charge from the electrodes is of great significance to achieve highly efficient OLEDs. A commonly used approach to reduce the barrier height for charge injection is to increase (decrease) the work function of the anode (cathode), toward the ultimate goal of achieving Ohmic contacts. Recently, transition-metal oxides, such as CuO, WO_3, MoO_3, and V_2O_5 have been shown to be promising candidates to replace the previous generation of organic hole injection layers at the anode, due to their stability, low cost, and their high work function.[1–4] It is this high work function ($\sim$5–6 eV), in particular, that has attracted the most attention since it suggests the possibility of forming an Ohmic contact for holes with many of the commonly used hole transport layers. However, a high work function does not guarantee an Ohmic contact or even good hole injection. For example, Au with a high work function of $\sim$5.1 eV will form a strong interfacial dipole at the metal/organic interface, which significantly increases the injection barrier for holes.[5] Therefore not only do we have to consider the work function of the oxides but we also have to take into account the energy-level alignment, for example, interfacial dipole effects. Previously, we have shown a theoretical framework to describe the energy-level alignment at metal/dielectric/organic interfaces using several arche-type oxides.[6–8] In order to better understand the physics that governs the injection process at such interfaces, particularly for the case of an Ohmic contact, a systematic study of different oxides used in devices is needed. However, few comparative studies have been conducted to study the injection properties of different oxides in devices, i.e., single-carrier hole-only devices. There may be a large variation in device performance from study-to-study and different processing methods and the organic materials used may introduce a large variation. It is therefore difficult to compare these results.

Several transition-metal oxides have been assumed to form an Ohmic contact with commonly used hole transporting molecules, such as N,N-diphenyl-N, N-bis-1-naphthyl-1–1-biphenyl-4,4-diamine (α-NPD).[9] With the assumption of Ohmic contacts, mobility of several organic semiconductors was extracted by modeling the current-voltage (*IV*) characteristics using the space-charge limited current (SCLC).[9,10] As will be shown in the following text, however, without clear criteria to distinguish between injection limited current (ILC) and SCLC, the data may easily be misinterpreted. For example, the square law, i.e., the Mott-Gurney law $J = \frac{9}{8}\varepsilon_0\varepsilon\mu\frac{V^2}{d^3}$, has been commonly used to analyze the *IV* characteristics of devices and has also been commonly cited as a criterion for SCLC.[11–15] However, such a criterion becomes questionable if the field-dependent mobility is unknown, as one can simply compare the *IV* characteristics to the quadratic relation. It is well known, however, that other effects such as nonuniform emission from a "patchy" interface,[16] the distribution of trap states in the bulk of the organic and the built-in potential,[17] will all change the shape of the *IV* characteristics. It is therefore extremely difficult to distinguish ILC from SCLC in organic devices from the *IV* characteris-

tics alone. Thus, any *IV* data analysis to extract parameters, such as the energy disorder and mobility of organics, are dubious without verification by other techniques. In this work we report the results of a comparative study between the most commonly used transition-metal oxides in organic electronic devices. These diverse experimental results enabled a thorough analysis of the various models relating to the injection properties at electrode/organic interfaces. To aid the analysis, time-domain simulations were used to establish a criterion to distinguish ILC from SCLC for α-NPD. As will be shown below there is no clear boundary between ILC and SCLC but rather a large region in between, which we will refer to as a "quasi-Ohmic" regime for the convenience of discussion. This intermediate quasi-Ohmic regime requires special consideration in terms of device modeling.

II. THEORY

A. Space-charge limited current

The maximum current that an organic semiconductor can sustain in the bulk (i.e., the amount of carriers in thermal equilibrium) is called the SCLC. An Ohmic contact is therefore an interface capable of injecting enough charges to sustain SCLC. One significant feature of SCLC is that the spatial distribution of electric field is $F(x) \propto x^{1/2}$, where x is the distance from the charge-injecting contact.[18] Therefore the electric field at an Ohmic contact is equal to zero, which, as will be shown, is an important criterion for distinguishing SCLC from ILC. Based on traditional semiconductor device physics, the SCLC for unipolar transport (i.e., single-carrier devices) in a perfect insulator (no intrinsic carriers) without traps is given by the Mott-Gurney law,[18]

$$J = \frac{9}{8}\varepsilon_0 \varepsilon \mu \frac{V^2}{d^3}, \tag{1}$$

where V is the applied voltage, d is the thickness of the film, and μ is the field-independent mobility. With a further consideration of an exponential tail of trap states, the *IV* characteristics based on Eq. (1) follows[18]

$$J \propto \mu \frac{V^{l+1}}{d^{2l+1}}, \tag{2}$$

where l is a parameter derived from the trap distribution. However, it is well known that the mobility for most organic semiconductors is field dependent. Also, in disordered organic materials, it is believed that all electronic states are localized and participate in conduction through thermally activated hopping, which yields a Poole-Frenkel-type field dependence of the mobility, i.e., $\mu(F) = \mu_0 \exp(\beta\sqrt{F})$. Under the assumption of the Poole-Frenkel dependence, an approximation to the SCLC for a field-dependent mobility is given by[19]

$$J_{\mathrm{SCLC}} = \frac{9}{8}\varepsilon\varepsilon_0\mu_0 \exp\left(0.89\beta\sqrt{\frac{V}{d}}\right)\frac{V^2}{d^3}. \tag{3}$$

Indeed, it has already been demonstrated that the above equation mathematically describes well the *IV* characteristics of many organic semiconductors.[20–22]

B. Injection limited current

When the current in an organic semiconductor is limited by the injection of charge from the electrode rather than the bulk properties of the material, it is called ILC. Under ILC conditions the spatial electric field distribution is assumed to be uniform, i.e., $F(x) = V/d$ whereas for SCLC the value of V/d only gives the average value of the electric field. This suggests that SCLC can be distinguished from ILC by the electric field at the charge-injecting contact [i.e., $F(x=0)=0$ for SCLC and $F(x=0)=V/d$ for ILC].

The most commonly used injection models for ILC are derived based on Richardson-Schottky (RS) emission,[23] Fowler-Nordheim tunneling,[24] and the hopping model.[25] It has been pointed out that RS emission is not strictly correct[26] for systems where the electron mean-free path is very short, such as in organic semiconductors. Although the hopping model includes the discrete (molecular) nature of organic semiconductors, it has also been pointed out that RS emission provides a solid basis for the analysis of the charge-injection characteristics of organic semiconductors since there is little quantitative difference between RS emission and the hopping model.[27,28] In this work we use the RS-emission-based model for ILC proposed by J. C. Scott. The model considers the scattering and diffusion effect by solving the drift-diffusion equation in the depletion zone of an amorphous semiconductor,[29]

$$J_{\mathrm{ILC}} = 4N_0\psi^2 e\mu F \exp\left(\frac{-e\phi_B}{k_B T}\right)\exp(f^{1/2}). \tag{4}$$

In Eq. (4), N_0 is the density of chargeable sites in the organic film, ϕ_B is the injection barrier height, F is the electric field at the charge-injecting contact, μ is the electric field dependent (Poole-Frenkel) carrier mobility, k_B is the Boltzmann constant, T is temperature, e is the electron charge, and ψ is a function of the reduced electric field ($f = e^3F/4\pi\varepsilon k_B^2T^2$),

$$\psi = f^{-1} + f^{-1/2} - f^{-1}(1 + 2f^{1/2})^{1/2}. \tag{5}$$

C. In between SCLC and ILC (quasi-Ohmic)

The two conditions discussed above, SCLC and ILC, correspond to the upper and lower limits, respectively. However, what about the case in between SCLC and ILC, when the electric field at the electrode contact is $0 < F(x=0) < V/d$? This indicates that there is in fact no clear boundary between SCLC and ILC but rather an intermediate regime in between. In other words, just because an *IV* characteristic is not ILC does not guarantee that it is SCLC and vice versa. Since the intermediate regime exhibits characteristics of both SCLC and ILC, it is incorrect to apply the models for either case [e.g., Eqs. (1)–(5)]. This can easily be understood since models for SCLC require that $F(x=0)=0$ at the charge-injecting contact while models for ILC require that $F(x=0)=V/d$ at the charge-injecting contact. Hence, for the region in between SCLC and ILC [i.e., $0 < F(x=0) < V/d$] neither type of model can be applied since the boundary conditions at the charge-injecting contact is not met. Therefore a new modeling approach is required in order to prop-

erly deal with the case between SCLC and ILC. From now on we will refer to this intermediate region as quasi-Ohmic, i.e., the current in the organic semiconductor is limited by both the injection at the electrode and by the bulk properties of the material.

Here, it is important to discuss the above definition of quasi-Ohmic. The term quasi-Ohmic has been misused in literature to describe the injection from a contact that is close enough to Ohmic so that the *IV* characteristics might be approximated by SCLC. However, this loose definition has often lead to physically meaningless analyses of *IV* characteristics using Eq. (1) or Eq. (3). Therefore, it is necessary to clearly define injection from a quasi-Ohmic contact in terms of the electric field at the charge-injecting contact [i.e., $0<F(x=0)<V/d$]. Based on this clear definition, we will show that the quasi-Ohmic regime is much larger (i.e., covers a greater range of injection barrier height) than has previously been expected. Moreover, it is important to note that the boundaries of the quasi-Ohmic regime are dependent on the field-dependent carrier mobility μ, the injection barrier height ϕ_B, the applied voltage V, and the device thickness d. As a result the same electrode contact (i.e., anode/organic interface) may display characteristics of ILC, quasi-Ohmic, and SCLC in different ranges of applied bias. This has significant implications for device modeling since most metal/organic interfaces used in real devices are found to fall into the quasi-Ohmic regime at typical operating voltages.

As discussed above, the quasi-Ohmic regime in between SCLC and ILC cannot be described using traditional models for SCLC or ILC. As a result a new approach that includes both the injection at the interfaces and the transport in the bulk of the organic is required to deal with this special case. Based on the transport models developed for inorganic semiconductors, i.e., the drift-diffusion and Poisson equations, we can conduct a time-domain simulation to study the distribution of electric field and carriers at steady state. This method has been employed by Scott *et al.*[30,31] to study the charge-injection and transport properties in single-layer OLEDs. Here, based on a similar theoretical framework, we conducted a simulation of single-carrier hole-only devices[32] to study quasi-Ohmic injection and to define a clear criterion to distinguishing SCLC from quasi-Ohmic and ILC.

In the simulation, space x and time t are discrete. The injection current density described by Eqs. (4) and (5) serves as a boundary condition at $x=0$, $t>0$ (i.e., the charge-injecting contact). The time-dependent continuity equation follows

$$\frac{\partial p(x,t)}{\partial t} = -\frac{1}{e}\frac{\partial J(x,t)}{\partial x}, \tag{6}$$

where p is the total density of holes and J is the conduction current density. The relation between the electric field and the charge density can be expressed by the Poisson equation as

$$\frac{\varepsilon_r \varepsilon_0}{e}\frac{\partial F(x,t)}{\partial x} = p(x,t). \tag{7}$$

In Eq. (7) ε_r and ε_0 are the dielectric constant of the organic and the dielectric permittivity in vacuum, respectively. The conduction current density can be calculated through the drift-diffusion equation,

$$J(x,t) = ep(x,t)\mu(F)F - eD\frac{\partial p(x,t)}{\partial x}, \tag{8}$$

where D is the diffusion coefficient, which can be obtained from Einstein's relation (as a function of the field-dependent mobility),

$$D = \frac{\mu k_B T}{e}. \tag{9}$$

The other boundary conditions for Eqs. (6)–(9) are

$$\begin{cases} V = \int_0^d F\ dx \\ F(x,t=0) = V/d \\ p(x,t=0) = 0 \\ J(x,t=0) = 0 \end{cases}, \tag{10}$$

where d is the thickness of the film and V is the applied voltage. It is noted that the transient current density J_t is contributed by the displacement current and the response of the charge-carrier density as

$$J_t(x,t) = \varepsilon_r \varepsilon_0 \frac{\partial F(x,t)}{\partial t} + J(x,t). \tag{11}$$

From Eq. (11) the total transient current at $x=d$ can be calculated until the steady state is reached. Also, the spatial distribution of electric field at steady state can be obtained from the simulation. From these simulation results the boundaries of the quasi-Ohmic regime (i.e., the lower limit of SCLC and the upper limit of ILC) can then be defined in terms of the electric field at the charge-injecting contact. Clearly, the boundaries of the quasi-Ohmic regime are dependent on the field-dependent carrier mobility μ, the injection barrier height ϕ_B, the applied voltage V, and the device thickness d.

Finally, it is noted that based on the results of Monte Carlo simulations, a criterion has been previously proposed to distinguish SCLC from ILC in organic semiconductors.[33] However this criterion does not take the field-dependent mobility into consideration, i.e., the criterion should be dependent on the applied electric field and should be different for different organic semiconductors. Moreover, the dependence of the film thickness has not been taken into account either. It is well known that the thicker the organic layer, the easier the injection will reach the SCLC since less charge can be sustained in the bulk. Here we will present a criterion for defining the boundaries of the quasi-Ohmic regime as a function of both the injection barrier height and film thickness for α-NPD by conducting a time-domain simulation under Eqs. (4)–(11).

III. EXPERIMENT

Single-carrier hole-only devices with a structure of anode/organic/cathode were used in this work. The devices were

fabricated in a Kurt J. Lesker LUMINOS® cluster tool with a base pressure of $\sim 10^{-8}$ Torr. Sample preparation consisted of substrate treatments and the deposition of metal, oxides, and organic layers on the substrates. The size of the substrates used, both Corning® 1737 glass and commercially patterned indium tin oxide (ITO) coated glass (with a sheet resistance less than 15 $\Omega/\square$), was 50 mm $\times$ 50 mm. Substrates were cleaned with a standard regiment of Alconox®, acetone, and methanol followed by UV ozone treatment for 15 min.

Ni, Cu, Co, Ag, and Au were thermally deposited in a dedicated metallization chamber from alumina-coated molybdenum boats. Tungsten trioxide (WO_3) and molybdenum trioxide (MoO_3) were thermally evaporated from tungsten boat and alumina-coated molybdenum boat, respectively. Vanadium pentoxide (V_2O_5) was deposited using radio frequency (rf) magnetron sputtering in a dedicated sputtering chamber with an rf power of 150 W in 1 mTorr Ar. It is noted that WO_3, MoO_3, and V_2O_5 were *in situ* deposited on the ITO substrates, then transferred to the organic deposition chamber without breaking vacuum ($\sim 10^{-9}$ Torr). Whereas, the Ni_2O_3, Co_3O_4, and CuO films were fabricated from pure Ni, Co, and Cu films, respectively, by *ex situ* oxidation using UV ozone for 30 min. Cu_2O films were also prepared by *ex situ* oxidation on a hot plate at 100 °C for 1 h. For the UV ozone treated samples (i.e., Ni_2O_3, Co_3O_4, and CuO) similar results were obtained for *in situ* oxidized films using O_2 plasma (without breaking vacuum), which indicates that any possible atmospheric contaminates play a negligible role in device performance.

The organic layer (α-NPD) was deposited in a dedicated organic chamber without breaking vacuum. The top cathode contact (Au or Ag) were deposited in the same dedicated metallization chamber as the anodes, without breaking vacuum. Au and Ag were chosen as the cathode contact metals to block electron injection and were found to yield nearly equivalent *IV* characteristics.[32] Devices were defined by the intersection of the top cathodes and the bottom anodes. The active area for all devices was 2 mm^2. The film thicknesses were monitored by a calibrated quartz-crystal microbalance and were further verified for each sample by using both a stylus profilometer (KLA Tencor P-16+) and capacitance-voltage (*CV*) measurements (Agilent 4294A). *IV* characteristics were measured in a closed loop He variable-temperature cryostat[32] with a base pressure of $\sim 10^{-7}$ Torr using an HP4140B picoammeter. All experimental results were verified for multiple devices on the same substrate and for the same device structure from different runs.

For the thermally deposited oxides, i.e., MoO_3 and WO_3, the injection is dependent on the thickness of the oxide layer. The thicknesses of the MoO_3 and WO_3 were optimized to 0.5 and 5 nm, respectively, which is consistent with previous reports in the literature.[9,34,35] It is also important to note that MoO_3 and WO_3 have a much worse reproducibility from system-to-system than the other oxides. It is well known that these oxides easily form bronzes with various atomic interstitials.[36] As a result the material properties of MoO_3 and WO_3 are highly unstable and are easily influenced by extremely subtle variations in processing conditions (e.g., even a slight change in base pressure can result in an entirely different oxide bronze).[37] This is evidenced, for example, by the wildly different performance of WO_3 reported in the literature.[34,35]

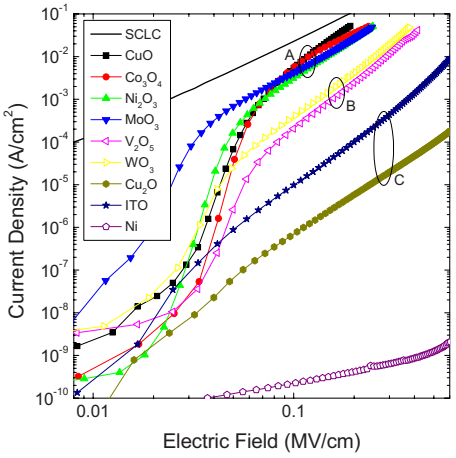

FIG. 1. (Color online) Current density (J) as a function of average electric field ($F=V/d$) for single-carrier hole-only devices with different metal oxide anodes at room temperature (297 K). The structure of the devices is anode/α-NPD ($\sim$500 nm)/Au. The solid line is the calculated SCLC from Eq. (3) for α-NPD using the field-dependent mobility we measured by the TOF technique and reported previously in Ref. 39. Notice that the different oxides fall into three different groups in terms of the current-voltage (*IV*) characteristics.

IV. RESULTS AND DISCUSSION

A. *IV* characteristics

Figure 1 compares the *IV* characteristics of α-NPD single-carrier hole-only devices with different oxide anodes and ITO at room temperature (297 K). The device structures are anode/α-NPD ($\sim$500 nm)/Au. Here Au is used as the cathode to block electron injection.[32] In order to eliminate any possible run-to-run difference in the organic layer thickness, we measured the organic layer thickness for each device and plotted the *IV* characteristics as a function of electric field. Also, the device thickness was chosen as 500 nm to minimize any effects of built-in potential at high electric field. The average electric field is taken as $F=V/d$, where d is the device thickness. The results for a pure Ni metal anode with high injection barrier height[38] is also shown for comparison. The device performance can be divided into three distinct groups: (A) CuO, Co_3O_4, Ni_2O_3, and MoO_3; (B) V_2O_5 and WO_3; and (C) ITO and Cu_2O. As we can see from the figure, the first group performs the best; the current density is almost one order of magnitude higher than for the second group and nearly three orders of magnitude higher than the ITO device.

The theoretical SCLC, calculated using Eq. (3) from the field-dependent mobility we measured by the time-of-flight (TOF) technique and reported previously in Ref. 39, is also shown in Fig. 1 (solid black line) as the upper limit of the *IV* characteristics. Indeed, the group A oxides approach this upper limit at high electric field, which would suggest that they

might be close to forming an Ohmic contact with α-NPD. As discussed in Sec. II, this case has traditionally been dealt with by assuming that the injection is close enough to an Ohmic contact that the current can be approximated by the SCLC. However, as we will show none of the oxides studied in this work were found to form an Ohmic contact with α-NPD (over the studied range of applied voltage), despite previous reports to the contrary. This discrepancy is due to the erroneous application of the Mott-Gurney law [i.e., Eq. (1) or Eq. (3)] to model *IV* characteristics in the quasi-Ohmic regime between SCLC and ILC. The quasi-Ohmic regime is found to cover a significant range of injection barrier heights and is dependent on the applied voltage, which will be discussed in details in Sec. IV D.

B. Fitting *IV* characteristics and transport parameters

In traditional semiconductor physics the slope of the *IV* characteristics is often used to identify SCLC following the Mott-Gurney law [i.e., Eq. (1)]. This criterion has also been commonly used (incorrectly albeit) for organic semiconductors. For example, the device performance of MoO_3 shown in Fig. 1 is consistent with the data reported in Ref. 9. (i.e., the current density is equivalent at the same applied electric field), in which the contact between MoO_3 and α-NPD was reported to be Ohmic since a slope of 2 of the *IV* characteristics was achieved. However, as discussed in Sec. II the Mott-Gurney law given by Eq. (1) does not apply to organic semiconductors with a field-dependent mobility, such as α-NPD. Hence a slope of 2 of the *IV* characteristics does not indicate that SCLC has been obtained.

Since the mobility of α-NPD is field dependent, the slope of the *IV* characteristics for SCLC should not be exactly 2 but in fact larger [see Eq. (3)]. The theoretical SCLC for α-NPD was calculated (black solid line in Fig. 1) based on the field-dependent mobility data that we have reported elsewhere measured by the TOF method;[39] a slope of ~2.5 is obtained from the calculated curve at high electric field. However, as will be shown below, even a slope of ~2.5 of the *IV* characteristics is still not sufficient to indicate that SCLC has been obtained. It should be pointed out that the shape of the *IV* curve is influenced by many other effects such as traps, the built-in potential, and nonuniform patchy emission. The effects of built-in potential will be discussed in detail below. In any event, due to the convolution of injection and transport properties, combined with the other effects mentioned above, the *IV* characteristics are insufficient to determine whether the current density is SCLC. In other words it is extremely difficult if not impossible to identify an Ohmic contact from the *IV* characteristics alone.

Also, fitting the *IV* characteristics with an analytical equation for SCLC is another common mistake used to distinguish an Ohmic contact, and has also been inappropriately used to extract transport parameters, such as mobility. However, as discussed above the Mott-Gurney law given by Eq. (1) is not applicable to organic semiconductors since most have field-dependent mobility. Moreover, even the form of Eq. (3), which considers the field-dependent mobility, is only a necessary but not a sufficient condition for SCLC. In other words, a good mathematically *fit* to the data using Eq. (3) does not guarantee that SCLC has been achieved. As a result, transport parameters, such as mobility, extracted from merely fitting the *IV* characteristics are physically meaningless. A quantitative example to emphasize this point is shown in Fig. 2.

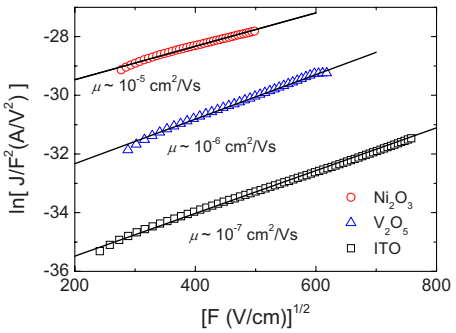

FIG. 2. (Color online) Current density (J) as a function of average electric field ($F=V/d$) for ITO/α-NPD, V_2O_5/α-NPD, and Ni_2O_3/α-NPD plotted as $\ln(J/F^2)$ vs $F^{1/2}$. The organic layer thickness (d) in all cases is ~500 nm. The linear fits are used to extract the apparent mobility from the current-voltage (*IV*) characteristics using Eq. (3). However, since a good fit is achieved for all three anodes, despite the significant difference in injection properties (see Fig. 1), the goodness of fit cannot be used to distinguish an Ohmic contact. What is more, the extracted mobility values are significantly different for each anode, and deviates significantly from the value we measured by TOF. This serves as an example that transport parameters cannot be extracted from *IV* characteristics, without verifying that a true Ohmic contact has been made using another technique.

Figure 2 shows the *IV* characteristics for Ni_2O_3 (group A), V_2O_5 (group B), and ITO along with the fitting results for SCLC using Eq. (3) following the same method as in Ref. 10. The data are linearized by plotting the *IV* characteristics in the form $\ln(J/F^2)$ versus $F^{1/2}$. For all three oxides an excellent linear fit is achieved, despite the significant difference in injection properties (see Fig. 1). Clearly, the goodness of mathematical fit cannot be used to distinguish SCLC. This point is further illustrated by the extracted mobility values, which are ~10^{-7}, ~10^{-6}, and ~10^{-5} cm^2/Vs extracted from ITO, V_2O_5, and Ni_2O_3 device, respectively. Clearly these values are all incorrect since a different value is obtained for the same organic semiconductor and all of which are orders of magnitude lower than the value we measured by TOF.[39]

Since the experiments were all conducted under the same well-controlled conditions, the possible system-to-system variation is eliminated. Furthermore, the thickness of the devices shown in Fig. 1 is almost the same, ~500 nm. As a result, the difference in injection current is not due to the apparent thickness-dependent mobility proposed by other works.[9,10] In any event, the results of Fig. 2 clearly demonstrate that a simple fit of the *IV* characteristics is insufficient to claim an Ohmic contact (SCLC), and furthermore any transport parameters extracted using this technique are in general incorrect. As discussed in Sec. II, the reason behind this incorrect analysis is the inappropriate assumption that the electric field at the charge-injecting contact is equals to

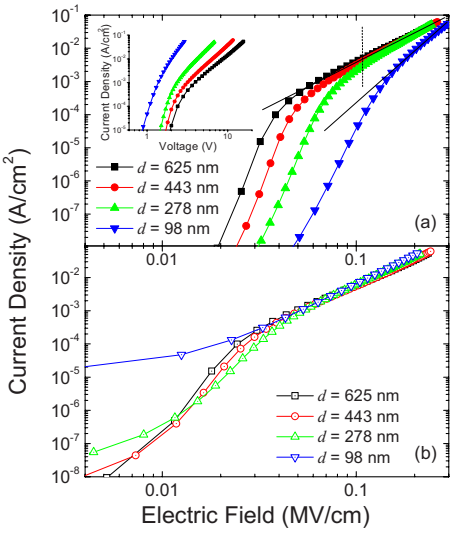

FIG. 3. (Color online) Current density (J) as a function of average electric field ($F=V/d$) for Ni_2O_3/α-NPD/Ag with different organic layer thicknesses (d) of α-NPD, of which (a) is before the subtraction of built-in potential (V_{bi}) and (b) is after subtraction of an estimated ~0.9 eV built-in potential. The inset of (a) is the current density as a function of voltage in the case of (a). Ag was chosen as cathode so as to increase the built-in potential.

zero, i.e., $F(x=0)=0$. Models for SCLC require that $F(x=0)=0$ as a boundary condition. However, as will be shown, for all of the examples in Fig. 2 the value of the electric field at the charge-injecting contact is much greater than zero. Clearly, the IV characteristics alone cannot be used to determine which models can be applied (e.g., SCLC, quasi-Ohmic, or ILC).

C. Built-in potential and device thickness dependence

Another common criterion used to identify SCLC is the thickness dependence of the IV characteristics. For ILC the voltage V is proportional to the device thickness d (i.e., $V \propto d$) at a fixed current density. While on the other hand, if the injection is bulk limited (SCLC), the thickness dependence becomes $V \propto d^x (1<x<1.5)$.[40] However, without knowledge of the exact value of the built-in potential it is difficult to distinguish between these two cases since the built-in potential also introduces an additional thickness dependence. This point is illustrated in Fig. 3, for Ni_2O_3 single-carrier hole-only devices with different organic layer thickness.

Figure 3(a) shows current density as a function of average applied electric field (i.e., $F=V/d$); the inset shows current density as a function of voltage. Clearly, the IV characteristics are different for each organic layer thickness, implying that the voltage is not proportional to the thickness, and hence the current is not ILC. However, if we subtract an estimated built-in potential (V_{bi}) of ~0.9 eV and replot the figure in Fig. 3(b), the IV characteristics [i.e., J vs $(V-V_{bi})/d$] are in good agreement for each organic layer thickness (i.e., $V \propto d$). This would suggest that the current is in fact ILC, in contrast to the previous analysis.

It is well known that the built-in potential cannot be simply calculated by the difference of work function between anode and cathode,[17] and it must be measured using other techniques, such as electroabsorption[41] and photovoltaic[17] measurements. For example, even a symmetric device with identical anode and cathode (e.g., Au/α-NPD/Au) does not necessarily have a zero built-in potential due to differences in the energy-level alignment between organic deposited on metal and metal deposited on organic. Regardless, without directly measuring the value of the built-in potential the thickness dependence of the IV characteristics is insufficient to claim an Ohmic contact. We also have to point out that even experimental determination of the exact value of the built-in potential in organic devices remains controversial.

Alternatively, one strategy to reduce the influence of the built-in potential is to increase the layer thickness of the organic so as to increase the applied bias for a given electric field strength. In this work all of the single-carrier devices were fabricated with a relatively thick (~500 nm) organic layer. As we have previously shown[32] this thickness is sufficient for α-NPD to negate any influence of the built-in potential at high electric field (the region where fitting is performed).

D. Criterion for SCLC, quasi-Ohmic, and ILC

As demonstrated in the previous sections, simple analytical equations cannot be directly applied to describe the IV characteristics of organic semiconductors without careful consideration. As of yet it is unclear what regime (i.e., SCLC, quasi-Ohmic, or ILC) the data shown in Fig. 1 falls into for each of the studied oxides. As discussed above the difficulty arises from the treatment of the quasi-Ohmic regime in between SCLC and ILC. We will therefore begin by defining the boundaries of the quasi-Ohmic regime (in terms of barrier height, device thickness, and applied voltage). In most cases, the quasi-Ohmic region is the most illusive (and most mistreated) region as one cannot use simple analytical equations for either the bulk limited current (SCLC) or ILC. For example, one cannot use the Mott-Gurney law given by Eq. (1) or Eq. (3) to analyze the IV characteristics since the electric field at the charge-injecting contact does not equal to zero [i.e., the Mott-Gurney law requires that $F(x=0)=0$]. Also, the data cannot be analyzed using the ILC models in this region either since $F \neq V/d$ at the interface, and the injection current has to be treated as one of the boundary conditions. A time-domain simulation that takes into account the dynamic nature of charge injection and transport is thus needed.

Figure 4 shows the simulated current density (solid symbols) as a function of applied voltage for a 500-nm-thick device. The dashed line is the ILC calculated using Eq. (4). The solid line is the calculated SCLC [from Eq. (3)] which defines a perfect Ohmic contact. As shown in the figure, the upper boundary of the simulated quasi-Ohmic regime with a 0.25 eV barrier height (solid triangles) converges with the Ohmic SCLC (black solid line). The lower boundary (~0.55 eV) of the simulated current is taken as the convergence of the ILC (dashed line) from Eq. (4) and the simula-

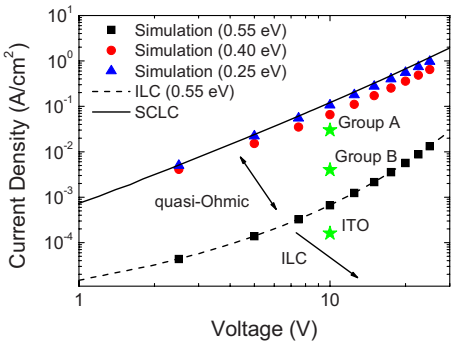

FIG. 4. (Color online) Current density (J) as a function of voltage (V) for different injection barrier heights (ϕ_{Bp}). The solid symbols correspond to the time-domain simulation results. The solid line is the calculated SCLC by Eq. (3) using the field-dependent mobility we measured by the TOF technique and reported previously in Ref. 39. The dashed line is the ILC calculated using Eq. (4). The current density at 10 V (i.e., $F=V/d=0.2$ MV/cm) for group A oxides, group B oxides, and ITO (see Fig. 1) is also shown as solid star symbols for comparison.

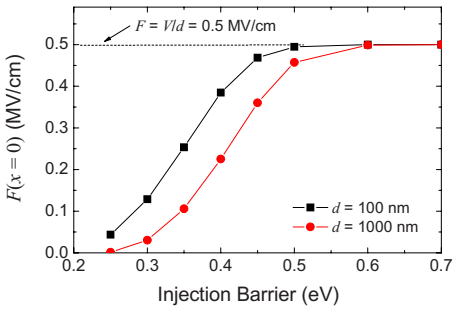

FIG. 5. (Color online) The calculated electric field at the charger-injecting contact [$F(x=0)$] as a function of barrier height (ϕ_{Bp}) for α-NPD with an organic layer thickness (d) of 100 and 1000 nm, respectively. The average electric field ($F=V/d$) for each case is 0.5 MV/cm. Notice that the electric field at the interface converges to the average value for increasing barrier height, and tends to zero for decreasing barrier height; the region in between defines a quasi-Ohmic contact.

tion results (solid squares). When the barrier height is larger than ~0.55 eV, the current density becomes strictly ILC, i.e., the bulk can support all of the injected charge, and hence the simulated current density and calculated ILC from Eq. (4) (dashed line and solid squares, respectively) are in excellent agreement. Therefore we can directly apply models for ILC to analyze the IV characteristics. It is clear that the quasi-Ohmic regime covers a significant range of current densities, and in fact includes both the group A and B oxides. The experimental results at an applied bias of 10 V ($F=V/d=0.2$ MV/cm) for the group A oxides, group B oxides, and ITO are also indicated in the figure. Clearly, ITO is the only example that yields ILC under these conditions.

As discussed above, the boundaries of the quasi-Ohmic regime were taken as the convergence of the simulation results with the SCLC from Eq. (3) and the ILC from Eq. (4). These boundaries represent the strict limits for SCLC and ILC in terms of the electric field at the charge-injecting contact [i.e., $F(x=0)=0$ for SCLC and $F(x=0)=V/d$ for ILC] as discussed in Sec. II. Figure 5 shows the calculated electric field at the charge-injecting contact (i.e., anode/α-NPD interface) as a function of the injection barrier height for two α-NPD layer thicknesses (same average electric field $F=V/d$). As we can see from the figure, the interfacial electric field depends strongly on the barrier height in the quasi-Ohmic regime. The interfacial electric field approaches zero as the barrier height is reduced to below ~0.25 eV, as expected. For high barrier >0.55 eV, the interfacial electric field reaches the average value (i.e., $F=V/d$) indicating the ILC regime. Figure 5 also shows that the transition among Ohmic, quasi-Ohmic, and ILC regimes depends on the device thickness. It is therefore critical to evaluate the effect of device thickness for various barrier heights.

Figure 6 is the calculated thickness-barrier height phase diagram for α-NPD devices at two nominal applied electric fields (i.e., $F=V/d$). Three regions can be defined on the figure, i.e., SCLC, quasi-Ohmic, and ILC. The solid symbols correspond to an average electric field of 0.5 MV/cm (the typical working electric field for OLEDs) while the open symbols to an average electric field of 0.1 MV/cm. Surprisingly, the quasi-Ohmic regime covers a significant portion of the phase diagram, and in fact encompasses the typical working range of injection barrier heights in real devices, such as OLEDs. It is also important to note that the boundaries of the quasi-Ohmic regime are strongly dependent on the average electric field (i.e., applied bias) as well. This is not surprising since the mobility and charge injection are dependent on electric field. As shown in Fig. 6 when the electric field increases from 0.1 to 0.5 MV/cm, the boundaries of the quasi-Ohmic regime significantly expand.

Since both the group A and B oxides fall into the quasi-Ohmic regime (for the device thickness and range of applied bias considered in this work) the time-domain simulation must be used to extract the injection barrier height (or mo-

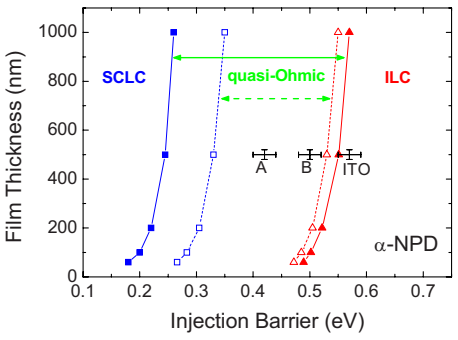

FIG. 6. (Color online) The calculated injection phase diagram for α-NPD indicating the boundaries of the quasi-Ohmic regime (i.e., the criterion for ILC and SCLC) as a function of the injection barrier height (ϕ_{Bp}) and the organic layer thickness (d). The first region (left side) defines the criterion for an Ohmic contact (SCLC), the second region (middle) is for a quasi-Ohmic contact, and the third region (right side) is for an ILC. The boundaries for these regimes are dependent on applied bias. The solid symbols correspond to an average electric field of 0.5 MV/cm while the open symbols to an electric field of 0.1 MV/cm. The results for the group A and group B oxides as well as ITO are also shown for comparison.

bility) by fitting the *IV* characteristics. The barrier heights for the group A and group B oxides as well as ITO are indicated in Fig. 6. Using this method the injection barrier height is estimated to be ~0.42 eV for the group A oxides (such as Ni_2O_3) and ~0.50 eV for group B oxide (such as WO_3). On the other hand, the injection from ITO into α-NPD is obviously injection limited; the barrier is estimated to be ~0.56 eV using Eq. (4). These values agree well with values independently extracted from ultraviolet photoelectron spectroscopy measurements, the details of which will be discussed elsewhere. Here we also have to note that the exact values of the barrier height may vary slightly for different injection models used as the boundary condition in the simulation. Also, although the time-domain simulation can describe the *IV* characteristics across all three regimes (i.e., SCLC, quasi-Ohmic, and ILC), simple analytic equations are preferable and convenient to describe SCLC and ILC due to the computational complexity of the time-domain simulation.

V. SUMMARY

In summary, the hole injection from different metal oxides into α-NPD has been systematically studied in single-carrier hole-only devices yielding a *IV* database for variable injection barrier heights. The device performance data is found to aggregate into three distinct groups: (A) CuO, Co_3O_4, Ni_2O_3, and MoO_3; (B) V_2O_5 and WO_3; and (C) ITO and Cu_2O. Based on the experimental results several key finds have been made.

First, it is found that none of the metal oxides studied in this work form a true Ohmic contact (SCLC) to α-NPD (over the practical range of applied bias used in devices), despite previous reports to the contrary. This discrepancy is attributed to incorrect data analysis in previous studies as a result of merely applying simple analytical equations for SCLC (e.g., Mott-Gurney) to evaluate the *IV* characteristics. Without prior knowledge of the field-dependent mobility, *IV* characteristics cannot be used to identify an Ohmic contact.

Second, it is found that there is no clear boundary between SCLC and ILC conditions but rather a large intermediate regime, namely, quasi-Ohmic, which includes characteristics of both. As a result, the *IV* characteristics in the quasi-Ohmic regime cannot be simply analyzed by either the bulk transport models (e.g., Mott-Gurney law) or the injection models. The boundaries of the quasi-Ohmic regime are defined by the electric field at the electrode contact [i.e., $0 < F(x=0) < V/d$].

Third, it is found that the quasi-Ohmic regime is surprisingly large and covers a wide range of barrier heights. Using a time-domain simulation of the transport of charge carriers across an organic semiconductor the boundaries of the quasi-Ohmic regime were evaluated as a criterion to distinguish SCLC from quasi-Ohmic and ILC. It is found that the *IV* characteristics for most electrode/organic contacts fall into the quasi-Ohmic regime. It is also found that the boundaries of the quasi-Ohmic regime have a strong dependence on the thickness of the organic layer and the applied bias.

Forth, it is found that the built-in potential can significantly distort the thickness dependence of the *IV* characteristics, particularly for organic layer thicknesses <100 nm. Without measuring the exact value of the built-in potential, a thicker organic layer of >500 nm is required to minimize the effects of any built-in potential on the *IV* characteristics.

Finally, an injection phase diagram for α-NPD has been shown as a case study to clearly demonstrate the above-mentioned effects. The group A and group B oxides discussed above are found to fall within the quasi-Ohmic regime while ITO is found to be purely injection limited. Using the time-domain simulation the injection barrier height for the various oxides has been deduced to be in the range of ~0.4 eV for group A oxides, ~0.5 eV for group B oxides, and ~0.6 eV for ITO. For other organic semiconductors with different field-dependent mobility a new phase diagram should be calculated.

ACKNOWLEDGMENTS

We wish to acknowledge funding for this research from Ontario Centres of Excellence and Natural Sciences and Engineering Research Council (NSERC) of Canada.

*Corresponding author; zhibin.wang@utoronto.ca
†zhenghong.lu@utoronto.ca

[1] G. B. Murdoch, M. Greiner, M. G. Helander, Z. B. Wang, and Z. H. Lu, Appl. Phys. Lett. **93**, 083309 (2008).
[2] C.-W. Chu, S.-H. Li, C.-W. Chen, V. Shrotriya, and Y. Yang, Appl. Phys. Lett. **87**, 193508 (2005).
[3] H. Kanno, R. J. Holmes, Y. Sun, S. Kena-Cohen, and S. R. Forrest, Adv. Mater. (Weinheim, Ger.) **18**, 339 (2006).
[4] Y. Han, D. Yanfeng, Z. Zhiqiang, and M. Dongge, J. Appl. Phys. **101**, 026105 (2007).
[5] N. Koch, A. Kahn, J. Ghijsen, J. J. Pireaux, J. Schwartz, R. L. Johnson, and A. Elschner, Appl. Phys. Lett. **82**, 70 (2003).
[6] M. G. Helander, Z. B. Wang, J. Qiu, and Z. H. Lu, Appl. Phys. Lett. **93**, 193310 (2008).
[7] M. G. Helander, Z. B. Wang, M. T. Greiner, J. Qiu, and Z. H. Lu, Appl. Phys. Lett. **95**, 083301 (2009).
[8] Z. B. Wang, M. G. Helander, M. T. Greiner, J. Qiu, and Z. H. Lu, Appl. Phys. Lett. **95**, 043302 (2009).
[9] T. Matsushima, Y. Kinoshita, and H. Murata, Appl. Phys. Lett. **91**, 253504 (2007).
[10] T.-Y. Chu and O.-K. Song, Appl. Phys. Lett. **90**, 203512 (2007).
[11] C. Ganzorig, M. Sakomura, K. Ueda, and M. Fujihira, Appl. Phys. Lett. **89**, 263501 (2006).
[12] N. Huby, L. Hirsch, G. Wantz, L. Vignau, A. S. Barriere, J. P. Parneix, L. Aubouy, and P. Gerbier, J. Appl. Phys. **99**, 084907 (2006).
[13] R. Agrawal, P. Kumar, S. Ghosh, and A. K. Mahaptro, Appl. Phys. Lett. **93**, 073311 (2008).
[14] P. W. M. Blom, C. Tanase, D. M. de Leeuw, and R. Coehoorn, Appl. Phys. Lett. **86**, 092105 (2005).

[15] M. Kiy, P. Losio, I. Biaggio, M. Koehler, A. Tapponnier, and P. Gunter, Appl. Phys. Lett. **80**, 1198 (2002).
[16] C. Herring and M. H. Nichols, Rev. Mod. Phys. **21**, 185 (1949).
[17] G. G. Malliaras, J. R. Salem, P. J. Brock, and J. C. Scott, J. Appl. Phys. **84**, 1583 (1998).
[18] M. A. Lampert and P. Mark, *Current Injection in Solids* (Academic, New York, 1970).
[19] P. N. Murgatroyd, J. Phys. D **3**, 151 (1970).
[20] S. W. Tsang, S. K. So, and J. B. Xu, J. Appl. Phys. **99**, 013706 (2006).
[21] C. H. Cheung, K. C. Kwok, S. C. Tse, and S. K. So, J. Appl. Phys. **103**, 093705 (2008).
[22] S. K. So, S. C. Tse, and K. L. Tong, J. Disp. Technol. **3**, 225 (2007).
[23] S. M. Sze, *Physics of semiconductor devices* (Wiley-Interscience, New York, 1981).
[24] R. H. Fowler and L. Nordheim, Proc. R. Soc. London **119**, 173 (1928).
[25] V. I. Arkhipov, E. V. Emelianova, Y. H. Tak, and H. Bässler, J. Appl. Phys. **84**, 848 (1998).
[26] J. G. Simmons, Phys. Rev. Lett. **15**, 967 (1965).
[27] V. I. Arkhipov and H. Bassler, Appl. Phys. Lett. **77**, 2758 (2000).
[28] U. Wolf, V. I. Arkhipov, and H. Bässler, Phys. Rev. B **59**, 7507 (1999).
[29] J. C. Scott and G. G. Malliaras, Chem. Phys. Lett. **299**, 115 (1999).
[30] G. G. Malliaras and J. C. Scott, J. Appl. Phys. **85**, 7426 (1999).
[31] G. G. Malliaras and J. C. Scott, J. Appl. Phys. **83**, 5399 (1998).
[32] M. G. Helander, Z. B. Wang, M. T. Greiner, J. Qiu, and Z. H. Lu, Rev. Sci. Instrum. **80**, 033901 (2009).
[33] U. Wolf, S. Barth, and H. Bassler, Appl. Phys. Lett. **75**, 2035 (1999).
[34] J. Li, M. Yahiro, K. Ishida, H. Yamada, and K. Matsushige, Synth. Met. **151**, 141 (2005).
[35] J. Meyer, S. Hamwi, T. Bulow, H. H. Johannes, T. Riedl, and W. Kowalsky, Appl. Phys. Lett. **91**, 113506 (2007).
[36] F. Wöhler, Ann. Chim. Phys. **29**, 43 (1823).
[37] Z. Hussain, Appl. Opt. **38**, 7112 (1999).
[38] Z. B. Wang, M. G. Helander, S. W. Tsang, and Z. H. Lu, Phys. Rev. B **78**, 193303 (2008).
[39] S. W. Tsang, M. W. Denhoff, Y. Tao, and Z. H. Lu, Phys. Rev. B **78**, 081301(R) (2008).
[40] M. A. Baldo and S. R. Forrest, Phys. Rev. B **64**, 085201 (2001).
[41] I. H. Campbell, T. W. Hagler, D. L. Smith, and J. P. Ferraris, Phys. Rev. Lett. **76**, 1900 (1996).